Enzyme-free amplified detection of cellular microRNA by light-harvesting fluorescent nanoparticle probes

Sylvie Egloff, Nina Melnychuk, Andreas Reisch, Sophie Martin, Andrey Klymchenko

Enzyme-free amplified detection of cellular microRNA by light-harvesting fluorescent nanoparticle probes

Sylvie Egloff, Nina Melnychuk, Andreas Reisch, Sophie Martin, Andrey S. Klymchenko*

Laboratoire de Bioimagerie et Pathologies, UMR 7021 CNRS, Faculté de Pharmacie, Université de Strasbourg, 74, Route du Rhin, 67401 Illkirch, France.

*Corresponding author. E-mail address: andrey.klymchenko@unistra.fr (A. S. Klymchenko); tel: +33 368 85 42 55.

Abstract

Detection of cellular microRNA biomarkers is an emerging powerful tool in cancer diagnostics. Currently, it requires multistep tedious protocols based on molecular amplification of the RNA target, *e.g.* RT-qPCR. Here, we developed a one-step enzyme-free method for microRNA detection in cellular extracts based on light-harvesting nanoparticle (nanoantenna) biosensors. They amplify the fluorescence signal by effective Förster resonance energy transfer (FRET) from ultrabright dye-loaded polymeric nanoparticle to a single acceptor and thus convert recognition of one microRNA copy (through nucleic acid strand displacement) into a response of >400 dyes. The developed nanoprobes of 17-19 nm diameter for four microRNAs (miR-21, let-7f, miR-222 and miR-30a) exhibit outstanding brightness (up to 3.8×10^7 $M^{-1}cm^{-1}$) and ratiometric sequence-specific response to microRNA with the limit of detection (LOD) down to 1.3 pM (21 attomoles), equivalent to 24 RT-qPCR cycles. They enable quantitative detection of the four microRNAs in RNA extracts from five cancerous cell lines (human breast cancer - T47D and MCF7, head and neck cancer - CAL33 and glioblastoma - LNZ308 and U373) and two non-cancerous ones (Hek293 and MCF10A), in agreement with RT-qPCR. The results confirmed that let-7f and especially miR-21 are systematically overexpressed in all studied cancerous cell lines. These nanoparticle biosensors are compatible with low-cost portable fluorometers and small detection volumes (11 attomoles LOD), opening a route to rapid point-of-care cancer diagnostics.

Keywords: Nanoparticle biosensors, Light-harvesting nanoantenna, MicroRNA detection, Cellular extracts, Cancer biomarkers, Point-of-care diagnostics.

1. Introduction

MicroRNA are small non-coding RNAs (18 to 25 nt) which inhibit gene expression at the post-transcriptional level, repressing mRNA translation with or without transcript degradation (Ebert and Sharp 2012; Hausser and Zavolan 2014; Krol et al. 2010). Almost 2000 microRNAs have been identified in the human genome since their discovery (Lee et al. 1993) and they are predicted to modulate more than 60 % of genes (Friedman et al. 2009) where a single microRNA can regulate hundreds of mRNA and thus govern an entire expression network (Pritchard et al. 2012; Treiber et al. 2019). Due to their vast regulatory role, abnormal microRNA expression levels are now studied as diagnostic biomarker for various diseases such as cancer, neurodegenerative diseases, diabetes, cardiovascular disease, kidney disease, liver disease, and even immune dysfunction (Chen et al. 2019; Gebert and MacRae 2019). In particular, differential expression of microRNA can be involved in cancer (Lu et al. 2005), where it has been identified as biomarker for diagnosis and prognosis of the disease, allowing, for example, evaluation of metastasis and chemoresistance (Hayes et al. 2014; Sohel 2020; Zhang et al. 2007). However, detection of microRNAs is challenging because they are short sequences in low abundance, they comprise only about 0.01 % of the total RNA and single microRNA levels differ widely from a few copies to >10,000 copies per cell (Bartel 2004; Dong et al. 2013).

To detect these low concentrations of microRNA in biological samples, molecular amplification strategies are employed (Figure 1A) (Chen et al. 2018; Dong et al. 2013). Currently, real-time quantitative polymerase chain reaction (RT-qPCR) is the golden standard technique for microRNA detection, in addition to microarray and northern blot techniques (Baker 2010; Chen et al. 2005; Mestdagh et al. 2014). However, RT-qPCR is based on complex time-consuming procedures using expensive reagents and it requires a specialized equipment and skilled personnel. To address these limitations, new methods relying on amplification strategies have been developed, notably isothermal exponential amplification (Deng et al. 2017) based on enzymes, including rolling circle amplification (RCA) (Ali et al. 2014; Lizardi et al. 1998), loop-mediated isothermal amplification (LAMP) (Notomi et al. 2000; Tomita et al. 2008), and specific high-sensitivity enzymatic reporter unlocking (SHERLOCK) (Gootenberg et al. 2018), or without enzymes, such as catalyzed hairpin assembly (CHA), (Yin et al. 2008) hybridization chain reaction (HCR) (Dirks and Pierce 2004; Hou et al. 2015), nucleic acid templated chemical reaction (Holtzer et al. 2016; Seckute et al. 2013), etc.

Nanomaterials offer new possibilities in the field of biodetection (Howes et al. 2014; Wolfbeis 2015), especially for detection of cancer biomarkers (Chinen et al. 2015). Gold nanoparticles (Alhasan et al. 2012; Coutinho and Somoza 2019), magnetic nanoparticles (Oishi and Sugiyama 2016), and luminescent nanomaterials, such as silver nanoclusters,(Shah et al. 2012; Yang and Vosch 2011) quantum dots (QDs) (Goryacheva et al. 2019; Qiu and Hildebrandt 2015), upconverting nanoparticles (Qu et al. 2019), fluorescent DNA nanoswitchers (Chandrasekaran et al. 2019), etc have been already developed to detect microRNA. In addition, rapidly developing photoelectrochemical techniques offer new possibilities in the design of nanomaterials for detection of molecular biomarkers in point-of-care settings (Shu and Tang 2020; Yu et al. 2019). Particularly promising are approaches where nanomaterials provide direct signal amplification, which was earlier shown for conjugated polymers (Jiang and McNeill 2017; Wu et al. 2017) and plasmonic gold-based nanostructures

(Acuna et al. 2012; Ochmann et al. 2017). The latter enabled to drastically improve the detection limits in standard bioassays for biomolecular markers (Luan et al. 2020). Although diverse design strategies for microRNA detection have been reported, most of the methods are blocked on the proof-of-concept step because of complicated multi-step fabrication of the sensor, batch-to-batch reproducibility and complex quality control protocols. Therefore, significant efforts are still required to integrate them into portable point-of-care devices (Dave et al. 2019).

An attractive approach to a simple and highly sensitive assay for RNA detection is to use ultrabright dye-loaded polymeric nanoparticles (NPs) (Reisch and Klymchenko 2016). These NPs feature controlled small size and exceptional brightness, because they encapsulate 100-10,000 dyes with their bulky counterions that prevent aggregation-caused quenching (Reisch et al. 2014; Reisch et al. 2018; Reisch et al. 2015). In these NPs, thousands of strongly coupled dyes can undergo efficient Förster Resonance Energy Transfer (FRET) to a single acceptor and thus operate as light-harvesting nanoantenna capable to amplify emission of single dye molecules >1000 fold, allowing for the first-time detection of single molecules in sunlight excitation conditions (Trofymchuk et al. 2017). These nanoantennas, functionalized with nucleic acids enable amplified detection of nucleic acids in solution and on surfaces down to single molecule sensitivity, being also compatible with serum-containing media (Melnychuk et al. 2020a; Melnychuk and Klymchenko 2018). Their ratiometric color response to an analyte allows smartphone-based detection of nucleic acids, attractive for point-of-care assays (Severi et al. 2020). However, so far, they have neither been designed for microRNA detection nor applied to biological samples.

Here, with the aim to drastically simplify the miRNA detection for point-of-care applications, we developed a robust method for direct enzyme-free detection of microRNA from cell lysates based on signal-amplifying light-harvesting nanoantennas. Four microRNA were selected, namely, miR-21 (Si et al. 2007; Yan et al. 2008), miR-222 (le Sage et al. 2007), Let-7f (Yan et al. 2008) and miR-30a (Baffa et al. 2009), which are known to be differently expressed in cancers. The developed nanoprobes, owing to their outstanding brightness and intrinsic signal amplification capability, enable high-sensitivity detection of microRNA targets in RNA extracts from seven cell lines and show compatibility with low-cost portable fluorometers, important for point-of-care diagnostics assays.

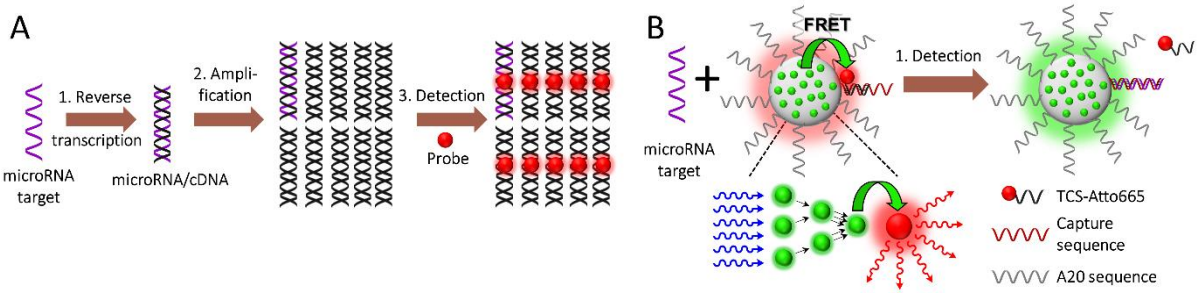

Figure 1. Strategies for microRNA detection. (A) Classical approaches (RT-qPCR, isothermal amplification, etc): microRNA target is first reverse transcribed into cDNA and then amplified to have enough target copies for the detection step. (B) Our strategy: the microRNA target is simply mixed with FRET nanoprobes followed by detection in one-step.

2. Results

2.1. Synthesis and characterization of nanoprobes

The nanoprobes for microRNA were designed based on a strand displacement mechanism (Simmel et al. 2019). At the surface of the dye-loaded nanoparticle (NP, FRET donor), the capture DNA oligonucleotide complementary to target miRNA is hybridized with the short target-competitive sequence (TCS) bearing FRET acceptor (TCS-Atto665, Figure 1B). This configuration generates FRET from NP to TCS-Atto665, leading to red emission of the acceptor. Then, addition of miRNA displaces TCS-Atto665, which blocks FRET, thus generating ratiometric response of the nanoprobe with emission color switching from red (acceptor) to green (donor, Figure 1B). The use of our light-harvesting nanoantenna particle as FRET donor should result in the signal amplification, because a single strand displacement triggers the response of 100-1000 of encapsulated FRET donor dyes (Melnychuk et al. 2020a; Melnychuk and Klymchenko 2018). To assemble the nanoprobes, dye-loaded polymeric NPs bearing azide reactive groups were first prepared by nanoprecipitation of a poly(ethyl methacrylate)-based polymer azide (PEMA-N3) with a corresponding dye salt (Figure 2A). The latter is composed of octadecyl rhodamine B (R18) with a bulky hydrophobic counterion (F5-TPB), which is required for preventing aggregation-caused quenching and ensuring effective energy transfer (Reisch et al. 2014; Trofymchuk et al. 2017). The obtained NPs (16 nm size according to DLS and TEM, Figure S1) were functionalized with a corresponding capture DNA-DBCO sequence (22-23mer), complementary to microRNA targets: miR-21, let-7f, miR-222, or miR-30a. We also added 59-fold excess of non-coding DNA-DBCO sequence (A20), in order to ensure dense DNA coating of NPs and strict control of the number of capture sequences per NP (Figure 2A). Then, the capture oligonucleotides were hybridized with corresponding TCS-Atto665, yielding the four final nanoprobes. The length of TCS oligonucleotide of 12-13 bases was designed to provide both stability of the duplex with the capture oligonucleotide at room temperature and efficient strand displacement by target microRNA.

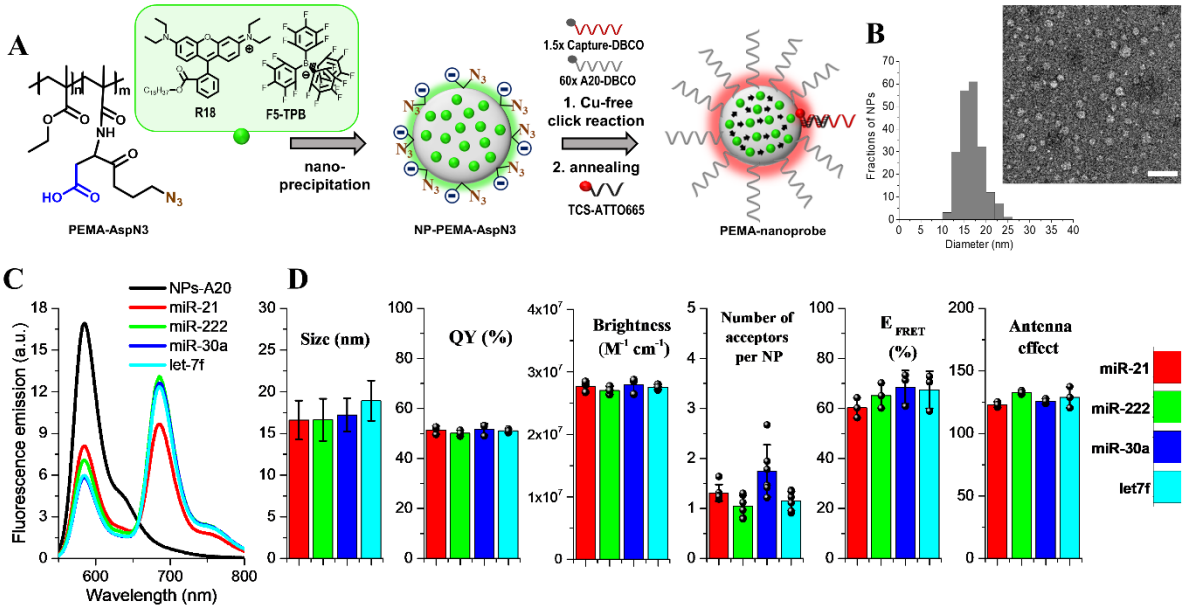

Figure 2. Characterisation of nanoprobes. (A) Synthesis scheme of nanoprobes. (B) Size by TEM for miR-222 (image and diagram of statistic distribution). Scale bar – 50 nm. (C) Fluorescence spectra of nanoprobes and control NPs-A20 without the acceptor. (D) Properties of nanoprobes (4 types of miR): Size by TEM (diameter, nm), number of acceptors per NP, quantum yield (QY, %), FRET efficiency (E_{FRET}) and Antenna effect (AE). For TEM, >200 NPs were analysed. Error bars are s.e.m. For optical properties, error bars are s.d.m (n = 3 for all data, except number of acceptors per NP, n = 6).

Transmission electron microscopy (TEM) revealed that they were all small (17-19 nm), independently of the used DNA coding sequences (Figure 2B, S1 and Table S1). Fluorescence spectroscopy showed that they all exhibited a characteristic two-band emission (Figure 2C), where the maximum around 580 nm corresponds to the FRET donor, while that at 680 nm – to the Atto665 FRET acceptor. All four probes exhibited high total fluorescence quantum yield combining donor and acceptor emission (QY = 50-52 %, Figure 2D), which together with the large number of encapsulated dyes (~400 per NP) implied high fluorescence brightness of nanoprobes ($2.7\text{-}3.8\times10^7$ $M^{-1}cm^{-1}$). The brightness per volume ratio (9400 $M^{-1}cm^{-1}nm^{-3}$) places them among the brightest fluorescent materials developed to date (Benson et al. 2020). Based on their absorption spectra (Figure S2), we estimated that all four nanoprobes bore approximately one acceptor per NP, exhibiting remarkably high FRET efficiencies, e.g. >60 % (Figure 2D). Due to efficient energy transfer from >400 encapsulated dyes to the single acceptor (TCS-Atto665) at the particle surface, the nanoprobes displayed a high antenna effect, which reached 130 (Figure 2D), according to the excitation spectra (Figure S2). The latter values correspond to the direct signal amplification, which together with high nanoprobe brightness, are required for amplified detection of nucleic acids.

2.2. Validation of nanoprobes with synthetic microRNA

The obtained nanoprobes were then evaluated in the presence of corresponding synthetic microRNA target. All four nanoprobes exhibited progressive decrease in the relative intensity of the acceptor with increasing microRNA target concentration (Figure 3A). This spectral response of the nanoprobes corresponds to the strand displacement of TSC-Atto665 by the microRNA target, leading to the FRET loss (Figure 1B). The logarithm of the FRET ratio, a semi-empirical parameter of FRET efficiency expressed as A/(A+D) was built vs miRNA concentration, where A and D were the pick intensities of the acceptor (at 665 nm) and the donor (at 580 nm), respectively. A clear concentration dependence for all four microRNA targets was observed, which could be fitted well with a linear regression (Figure 3B, Table S2). Based on the fitting parameters and the standard deviation of the control without the target, we estimated the limit of detection (LOD) for the nanoprobes to lie between 1 and 4 pM, depending on the probe (Figure 3B). As we used relatively low detection volume (16 µL), the LOD expressed in total amount of microRNA was as low as 21-29 attomoles in case of let-7f, miR-222 and miR-30a (Figure 3B). All four nanoprobes responded exclusively to their microRNA target and not to the other three tested microRNAs (Figure 3C and S3), indicating that the response of the nanoprobes was sequence specific. Moreover, the fluorescence spectra of the nanoprobe (miR-222, Figure S4) remained identical for 0, 1, 3 and 6 hours of incubation without the target, indicating remarkable stability of the FRET signal.

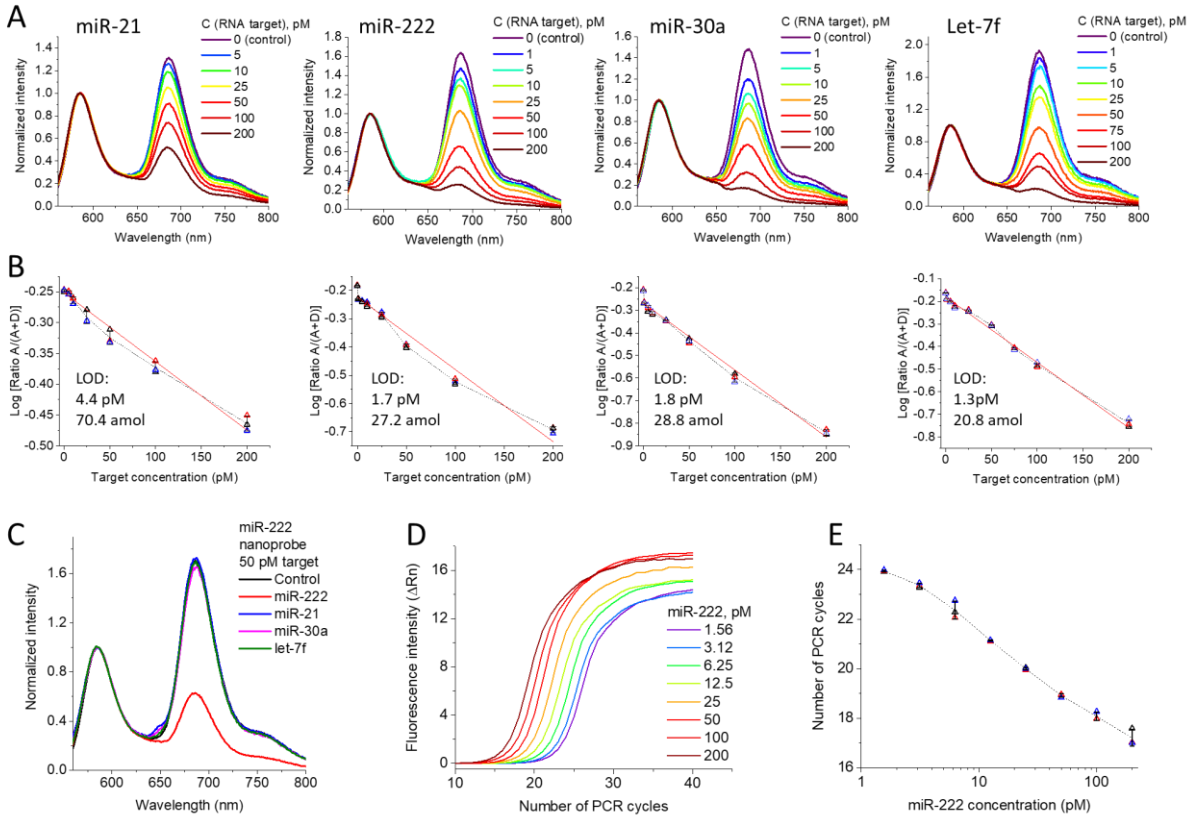

Figure 3. Validation of nanoprobes with synthetic RNA and their calibration. (A) Normalized fluorescence spectra of miR-21 (incubation for 6 hours at 30 °C), miR-222, miR-30a and let-7f probes (100 pM) after incubation for 6 hours at 20 °C, without (NPs) and with corresponding RNA target ranging from 1 to 200 pM. Excitation wavelength was 530 nm. (B) Calibration curves for each microRNA probes with linear fit (red line) and corresponding LOD (concentration and absolute amount). (C) Sequence-specificity of Specificity of miR-222 nanoprobe: incubation of miR-222 nanoprobes with 50 pM of each RNA target during 6 hours at 30 °C for miR-21 probes and at 20 °C for miR-222, miR-30a and let-7f probes. (D) Amplification curve for RT-qPCR for miR-222 synthetic target from 6 to 200 pM. (E) Correlation between number of cycles (RT-qPCR) and initial concentration of the miR-222 target (in triplicate). Error bars are s.d.m. (n = 3).

To understand better the level of sensitivity of our nanoprobes, we performed detection of synthetic miR-222 at different concentrations using RT-qPCR. As expected, the PCR curves shifted towards higher number of cycles with decrease in the miR-222 concentration (Figure 4D). Importantly, 1.56 pM concentration of miR-222, which was close to LOD of our nanoprobe, corresponded to ~24 PCR cycles (Figure 4E). This result suggests that the sensitivity of our microRNA probe, corresponding to 24 PCR cycles, is in the biologically relevant range for microRNA detection.

2.3. Testing nanoprobes in cell lysates

Having validated our new nanoprobes on synthetic microRNA targets, we moved to microRNA detection in cell lysates. To this end, we first performed RT-qPCR on fourteen cancer cell lines in order to select those where all four microRNA biomarkers vary to a significant extent (Table S3). Five cell lines were selected, representative of different cancers: human breast cancer (T47D and MCF7), head and neck cancer (CAL33) and glioblastoma (LNZ308 and U373). We also included two healthy cell lines (Hek293 and MCF10A) with good variability of these four biomarkers (Table S4). To realize microRNA detection with our nanoprobes, we performed RNA extraction from the cell lysates, as for RT-qPCR experiments (Figure 4A). The obtained total RNA extracts were mixed with the nanoprobes, while keeping minimal volume of the reaction mixture (16 µL) in order to ensure maximal speed of the strain displacement process (Figure 4A). After incubation for 6 hours, the mixture was diluted to 50 µL and measured in micro-cuvettes using a spectrofluorometer. It was found that for all four nanoprobes the decrease in the relative intensity of the long-wavelength FRET band depended strongly on the cell line (Figure 4B). The two-band spectral profiles for all four nanoprobes in both cancer (Figure S5) and healthy (Figure S6) cells lines were highly reproducible, indicating that the nanoprobes can provide robust signal for ratiometric quantification.

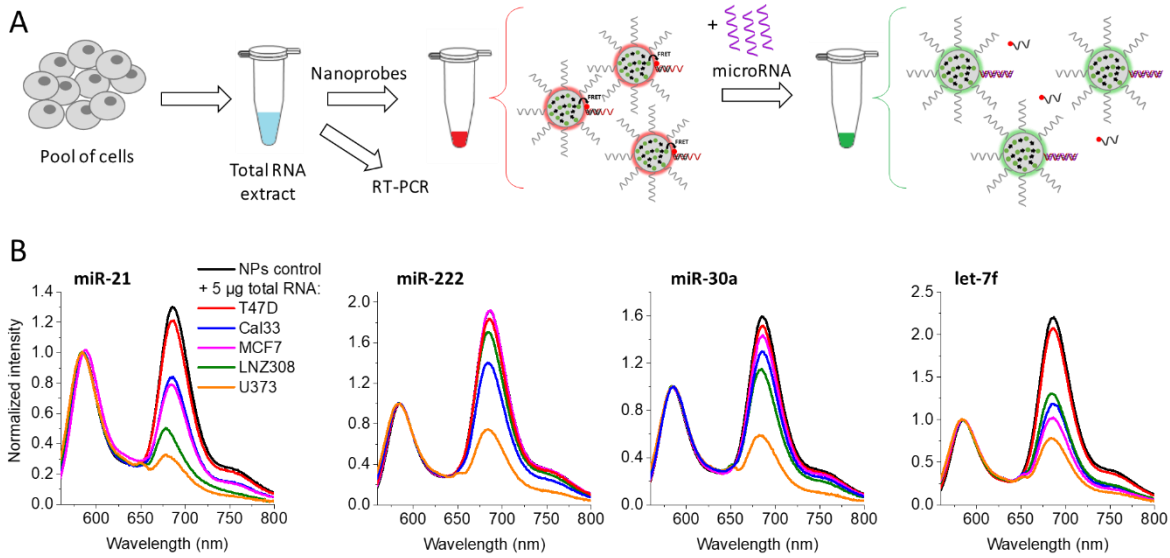

Figure 4. Detection of microRNA target in total RNA extracted from cells. (A) Principle of detection with the golden standard technique RT-PCR versus our concept with nanoprobes. (B) Normalized fluorescence spectra of miR-21(30 °C), miR-222, miR-30a and let-7f probes (100 pM) after incubation of 6 hours at 20 °C, without target (NPs) and with 5 µg of total RNA extract for 5 cancerous cell lines. Excitation wavelength was 530 nm.

To make a quantitative analysis with our nanoprobes, we used their corresponding calibration curves from Figure 3B. The latter allowed us to convert FRET ratio values observed in a given cellular RNA extract into the absolute concentration of microRNA (Figure 5). To ensure that our approach reflected the abundance of microRNA in the cell lysates, RT-qPCR analysis was performed for the four microRNAs in the same RNA extracts from seven studied cell lines (Figure 5A). In this case, the relative quantification (RQ) of microRNA by RT-qPCR was realized using an internal reference gene (RNU44**)**. The microRNA concentrations obtained by

the four nanoprobes correlated with relative amount of microRNA estimated by RT-qPCR for all seven cell lines. Indeed, RT-qPCR of U373 confirmed large abundance of all four microRNA biomarkers, whereas the lowest abundance in miR-21, miR-30a and let-7f was observed for T47D (Figure 5A). It should be noted that the correlation between the two methods was not perfect, which is clearly related to the different nature of the two methods. In case of RT-qPCR, relative quantification is carried out on reversed transcribed cDNA and is done with respect to an internal reference gene, whereas our method provides direct quantification of absolute concentration microRNA in the RNA extracts. Moreover, we cannot exclude that the presence of RNA extract from a cell lysate can affect accuracy of our method. Overall, direct comparison of the nanoprobes with RT-qPCR validates our method for microRNA detection in the RNA extracts from the cell lysates.

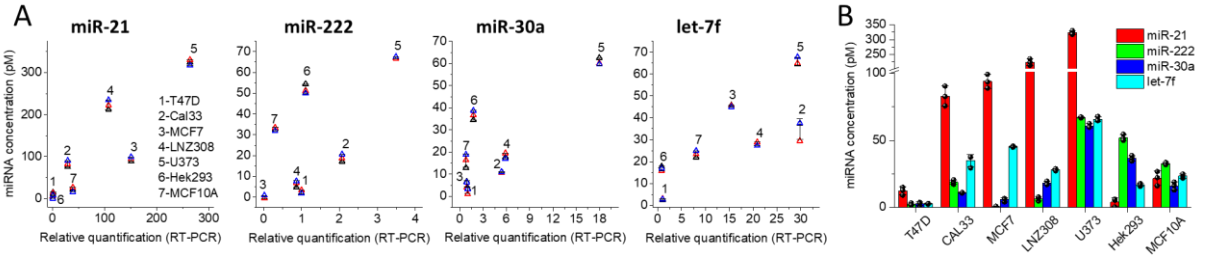

Figure 5. Quantification of microRNA in cells and correlation with RT-qPCR data. (A) Correlation between concentration of microRNA target obtained by nanoprobes versus relative quantification from RT-qPCR (RNU44 as reference) for 7 cell lines. Errors are s.d.m. (n = 3). (B) A fingerprint of microRNA expression for 7 cell lines based on the data from (A). Errors are s.d.m. (n = 3).

Then, we compared the abundance of the four microRNA biomarkers within the seven cell lines (Figure 5B). It can be seen that each cell line presented a unique combination of microRNA concentrations, like a "fingerprint". As a general trend, all cancer cell lines showed significantly higher concentration of miR-21 compared to other microRNAs, whereas in healthy cell lines, miR-21 concentration was similar or lower. Let-7f was also abundant in four out of five cancer cell lines, while being less important in healthy cells (and T47D cancer cell line). Moreover, miR-222 and miR-30a showed dramatic variations in different cell lines (Figure 5B), suggesting that they are also important for distinguishing cancer cells. Thus, using our method we can directly assess the microRNA fingerprint of cells and thus potentially identify the type of cancer. Taking into account that standard RNA extraction in our case generates ~60 µg of total RNA and we use 3×5 µg of total RNA for detection of one microRNA biomarker, our method can measure all four markers from a single RNA extraction.

2.4. Compatibility of the nanoprobe method with low-cost portable devices

We further studied compatibility of our nanoprobes with portable low-cost fluorescence detection devices (Figure 6): (i) Nanodrop^{TM} 3300 (Thermofisher Scientific), which can measure in a small sample volume (1-2 µL) and (ii) QFX (DeNovix), which makes detection directly in PCR tubes. Our tests using synthetic miR-222 showed good correlation of the FRET ratio vs miR-222 concentration, with limits of detection for both devices around 5 pM (Figure 6). Thus, our nanoprobes are compatible with both portable devices. Owing to the low detection

volumes, Nanodrop™ allowed us to further decrease the limit of detection down to 11 attomoles of microRNA. The latter means that we can further decrease the consumption of the sample by ~3-fold and thus measure from one RNA extraction >10 microRNA markers, which is highly attractive for development of point-of-care multiplexed assays.

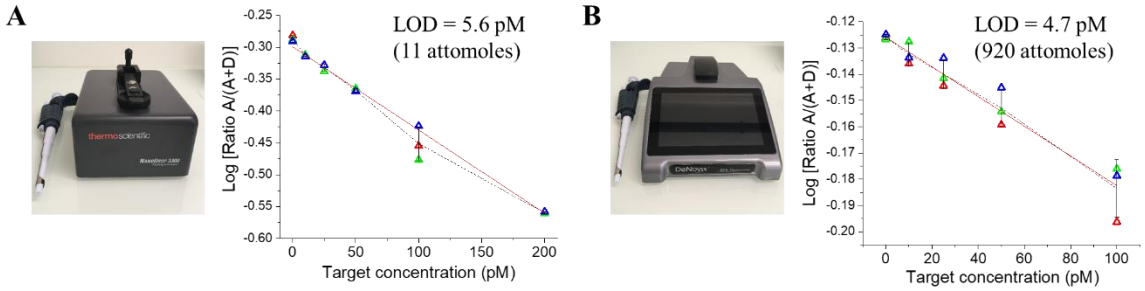

Figure 6. Nanoprobe performance using portable instruments. Incubations of nanoprobe miR-222 with its target RNA and further fluorescent measurements using portable fluorimeters (A) Nanodrop™ 3300 (ThermoFisher scientific) and (B) QFX (DeNovix). In case of Nanodrop™, incubations were done in the same conditions as described before and measurements was performed in a drop of 2 µL. Error bars are s.d.m (n = 7). In case of QFX, the incubation was done in a 200 µL, using same experimental conditions as before. The sample was measured as it is in thin-walled PCR tube. Error bars are s.d.m (n = 3).

3. Discussion

Current methods for detection of microRNAs in medical diagnostics rely on molecular amplification of the target (e.g. RT-qPCR, isothermal amplification, etc), because abundance of microRNA in biological/clinical samples is very low. In comparison to existing techniques for microRNA detection, our nanoantenna-based technology occupies a unique position. On one hand it is complementary to existing molecular amplification techniques based on enzymes, such as RT-qPCR (Mestdagh et al. 2014), RCA (Ali et al. 2014; Lizardi et al. 1998), LAMP (Notomi et al. 2000; Tomita et al. 2008) and SHERLOCK (Gootenberg et al. 2018), or those without enzymes, such as CHA (Yin et al. 2008) and HCR (Dirks and Pierce 2004; Hou et al. 2015). Our method does not require the amplification circuits as it exploits direct optical amplification based on light-harvesting nanoantenna (Trofymchuk et al. 2017) and thus, it is easier to use. Indeed, compared to RT-qPCR, our one-step detection method does not require reverse transcription and enzymatic amplification through a thermal cycling. However, the current limitation of our method compared to RT-qPCR is lower sensitivity (picomolar range), although it is possible to detect single nucleic acid copy by our nanoprobes using microscopy (Melnychuk et al. 2020b). On the other hand, as it is a homogeneous assay, it differs from emerging ultrasensitive techniques for microRNA detection, including surface plasmon resonance, electroluminescence, electrochemistry, optical microscopy, etc, which generally use rather complex surface-immobilization strategies (Dong et al. 2013; Xue et al. 2019). Then, the FRET-based operation principle in our nanoprobes provides a robust ratiometric signal readout, which is advantageous compared to single-channel intensity measurements. These features make our nanoprobes compatible with practically any existing fluorescence instruments, including spectrometers, plate readers, microscopes as well as miniaturized fluorometers presented in this work. Moreover, detection volumes can be further miniaturized with help of

microfluidic devices, which can further decrease the detection limit and simplify the detection, important for point-of-care assays (Gong and Sinton 2017; Shu and Tang 2020; Zhang et al. 2017).

4. Conclusion

Here, we propose a new methodology to measure microRNA in cell extracts based on DNA-functionalized light-harvesting nanoantenna, which couples a single molecular recognition event with the response of >400 highly emissive dyes. Nanoprobes for microRNA biomarkers of cancer (miR-21, let-7f, miR-222 and miR-30a) have been developed, featuring small size (17-19 nm), an outstanding fluorescence brightness due to 50-52 % fluorescence quantum yield and heavy dye loading (50 wt% vs polymer) as well as 130-fold antenna (amplification) effect. Experiments with synthetic microRNAs showed a sequence-specific ratiometric response of the nanoprobes to the target. The LOD of microRNA was 1.3 pM (21 attomoles in absolute amount), where 1.56 pM target corresponded to 24 cycles of RT-PCR, showing that the nanoprobes operate in the biologically relevant concentration range. The new nanoprobes enabled detection of the four microRNA in RNA extracts from cell lysates of 5 cancer and 2 healthy cell lines, showing correlation with RT-qPCR data. Based on the nanoprobe calibration with synthetic microRNA, direct quantification of microRNA in cells lysates was achieved by a simple protocol that does not require any enzymatic amplification step. The nanoprobes revealed a characteristic concentration profile of the four biomarkers (fingerprint) for each cancer cell line. We also found that miR-21 and to a lower extent let-7f were particularly abundant in cancer cell lines compared to the healthy ones, in line with earlier reports (Si et al. 2007; Yan et al. 2008). Finally, the new method was compatible with portable fluorescence devices, especially Nanodrop^{TM}, which allowed decreasing the sample volume, thus further improving the LOD to 11 attomoles.

Thus, owing to their intrinsic capacity to amplify the fluorescence signal, our nanoprobes provide a robust methodology for microRNA detection in biological samples, featuring high sensitivity and sequence specificity, simple one-step detection protocol, and compatibility with portable devices. These properties make them good candidates for the development of next generation point-of-care assays for molecular diagnostics. In the present form, the developed method is ready for clinical studies on microRNA detection in liquid biopsies from cancer patients.

Declaration of competing interest

Nina Melnychuk, Andreas Reisch and Andrey S. Klymchenko are inventors on a patent application related to this technology (European patent application no. 18305253.9). The remaining authors declare no competing interests.

Acknowledgements

This work was supported by the European Research Council ERC Consolidator grant BrightSens 648525 and SATT Conectus maturation grant NanoAntenna. We thank Corinne Crucifix from the FRISBI platform for her help with the electron microscopy.

Appendix A. Supplementary data

Supplementary data to this article can be found online at https://doi.org

References

Acuna, G.P., Moller, F.M., Holzmeister, P., Beater, S., Lalkens, B., Tinnefeld, P., 2012. Science 338, 506-510.

Alhasan, A.H., Kim, D.Y., Daniel, W.L., Watson, E., Meeks, J.J., Thaxton, C.S., Mirkin, C.A., 2012. Anal. Chem. 84, 4153-4160.

Ali, M.M., Li, F., Zhang, Z.Q., Zhang, K.X., Kang, D.K., Ankrum, J.A., Le, X.C., Zhao, W.A., 2014. Chem. Soc. Rev. 43, 3324-3341.

Baffa, R., et al., 2009. J. Pathol. 219, 214-221.

Baker, M., 2010. Nat. Methods 7, 687-692.

Bartel, D.P., 2004. Cell 116, 281-297.

Benson, C.R., et al., 2020. Chem 6, 1978-1997.

Chandrasekaran, A.R., MacIsaac, M., Dey, P., Levchenko, O., Zhou, L., Andres, M., Dey, B.K., Halvorsen, K., 2019. Science Advances 5, eaau9443.

Chen, C.F., et al., 2005. Nucleic Acids Res. 33, 9.

Chen, X., Xie, D., Zhao, Q., You, Z.H., 2019. Brief. Bioinform. 20, 515-539.

Chen, Y.X., Huang, K.J., Niu, K.X., 2018. Biosensors & Bioelectronics 99, 612-624.

Chinen, A.B., Guan, C.M., Ferrer, J.R., Barnaby, S.N., Merkel, T.J., Mirkin, C.A., 2015. Chem. Rev. 115, 10530-10574.

Coutinho, C., Somoza, A., 2019. Anal. Bioanal. Chem. 411, 1807-1824.

Dave, V.P., Ngo, T.A., Pernestig, A.K., Tilevik, D., Kant, K., Nguyen, T., Wolff, A., Bang, D.D., 2019. Lab. Invest. 99, 452-469.

Deng, R.J., Zhang, K.X., Li, J.H., 2017. Accounts Chem. Res. 50, 1059-1068.

Dirks, R.M., Pierce, N.A., 2004. Proc. Natl. Acad. Sci. U. S. A. 101, 15275-15278.

Dong, H.F., Lei, J.P., Ding, L., Wen, Y.Q., Ju, H.X., Zhang, X.J., 2013. Chem. Rev. 113, 6207-6233.

Ebert, M.S., Sharp, P.A., 2012. Cell 149, 515-524.

Friedman, R.C., Farh, K.K.H., Burge, C.B., Bartel, D.P., 2009. Genome Res. 19, 92-105.

Gebert, L.F.R., MacRae, I.J., 2019. Nat. Rev. Mol. Cell Biol. 20, 21-37.

Gong, M.M., Sinton, D., 2017. Chem. Rev. 117, 8447-8480.

Gootenberg, J.S., Abudayyeh, O.O., Kellner, M.J., Joung, J., Collins, J.J., Zhang, F., 2018. Science 360, 439-444.

Goryacheva, O.A., Novikova, A.S., Drozd, D.D., Pidenko, P.S., Ponomaryeva, T.S., Bakal, A.A., Mishra, P.K., Beloglazova, N.V., Goryacheva, I.Y., 2019. Trac-Trends Anal. Chem. 111, 197-205.

Hausser, J., Zavolan, M., 2014. Nat. Rev. Genet. 15, 599-612.

Hayes, J., Peruzzi, P.P., Lawler, S., 2014. Trends Mol. Med 20, 460-469.

Holtzer, L., Oleinich, I., Anzola, M., Lindberg, E., Sadhu, K.K., Gonzalez-Gaitan, M., Winssinger, N., 2016. ACS Central Sci. 2, 394-400.

Hou, T., Li, W., Liu, X.J., Li, F., 2015. Anal. Chem. 87, 11368-11374.

Howes, P.D., Chandrawati, R., Stevens, M.M., 2014. Science 346, 53-+.

Jiang, Y., McNeill, J., 2017. Chem. Rev. 117, 838-859.

Krol, J., Loedige, I., Filipowicz, W., 2010. Nat. Rev. Genet. 11, 597-610.

le Sage, C., et al., 2007. Embo J. 26, 3699-3708.

Lee, R.C., Feinbaum, R.L., Ambros, V., 1993. Cell 75, 843-854.

Lizardi, P.M., Huang, X.H., Zhu, Z.R., Bray-Ward, P., Thomas, D.C., Ward, D.C., 1998. Nature Genet. 19, 225-232.

Lu, J., et al., 2005. Nature 435, 834-838.
Luan, J., et al., 2020. Nature Biomedical Engineering 4, 518-530.
Melnychuk, N., Egloff, S., Runser, A., Reisch, A., Klymchenko, A.S., 2020a. Angew. Chem. Int. Ed. 59, 6811-6818.
Melnychuk, N., Egloff, S., Runser, A., Reisch, A., Klymchenko, A.S., 2020b. Angewandte Chemie-International Edition 59, 6811-6818.
Melnychuk, N., Klymchenko, A.S., 2018. Journal of the American Chemical Society 140, 10856-10865.
Mestdagh, P., et al., 2014. Nat. Methods 11, 809-815.
Notomi, T., Okayama, H., Masubuchi, H., Yonekawa, T., Watanabe, K., Amino, N., Hase, T., 2000. Nucleic Acids Res. 28, 7.
Ochmann, S.E., Vietz, C., Trofymchuk, K., Acuna, G.P., Lalkens, B., Tinnefeld, P., 2017. Anal. Chem. 89, 13000-13007.
Oishi, M., Sugiyama, S., 2016. Small 12, 5153-5158.
Pritchard, C.C., Cheng, H.H., Tewari, M., 2012. Nat. Rev. Genet. 13, 358-369.
Qiu, X., Hildebrandt, N., 2015. ACS Nano 9, 8449-8457.
Qu, A.H., Sun, M.Z., Xu, L.G., Hao, C.L., Wu, X.L., Xu, C.L., Kotov, N.A., Kuang, H., 2019. Proc. Natl. Acad. Sci. U. S. A. 116, 3391-3400.
Reisch, A., Didier, P., Richert, L., Oncul, S., Arntz, Y., Mely, Y., Klymchenko, A.S., 2014. Nature Communications 5, 4089.
Reisch, A., Heimburger, D., Ernst, P., Runser, A., Didier, P., Dujardin, D., Klymchenko, A.S., 2018. Advanced Functional Materials 28.
Reisch, A., Klymchenko, A.S., 2016. Small 12, 1968-1992.
Reisch, A., Runser, A., Arntz, Y., Mely, Y., Klymchenko, A.S., 2015. ACS Nano 9, 5104-5116.
Seckute, J., Yang, J., Devaraj, N.K., 2013. Nucleic Acids Res. 41, 9.
Severi, C., Melnychuk, N., Klymchenko, A.S., 2020. Biosens. Bioelectron. 168, 7.
Shah, P., Rorvig-Lund, A., Ben Chaabane, S., Thulstrup, P.W., Kjaergaard, H.G., Fron, E., Hofkens, J., Yang, S.W., Vosch, T., 2012. ACS Nano 6, 8803-8814.
Shu, J., Tang, D., 2020. Anal. Chem. 92, 363-377.
Si, M.L., Zhu, S., Wu, H., Lu, Z., Wu, F., Mo, Y.Y., 2007. Oncogene 26, 2799-2803.
Simmel, F.C., Yurke, B., Singh, H.R., 2019. Chem. Rev. 119, 6326-6369.
Sohel, M.M.H., 2020. Life Sci. 248, 12.
Tomita, N., Mori, Y., Kanda, H., Notomi, T., 2008. Nat. Protoc. 3, 877-882.
Treiber, T., Treiber, N., Meister, G., 2019. Nat. Rev. Mol. Cell Biol. 20, 5-20.
Trofymchuk, K., Reisch, A., Didier, P., Fras, F., Gilliot, P., Mely, Y., Klymchenko, A.S., 2017. Nature Photonics 11, 657-+.
Wolfbeis, O.S., 2015. Chem. Soc. Rev. 44, 4743-4768.
Wu, W.B., Bazan, G.C., Liu, B., 2017. Chem 2, 760-790.
Xue, T.Y., et al., 2019. Nature Communications 10, 28.
Yan, L.X., Huang, X.F., Shao, Q., Huang, M.Y., Deng, L., Wu, Q.L., Zeng, Y.X., Shao, J.Y., 2008. Rna 14, 2348-2360.
Yang, S.W., Vosch, T., 2011. Anal. Chem. 83, 6935-6939.
Yin, P., Choi, H.M.T., Calvert, C.R., Pierce, N.A., 2008. Nature 451, 318-U314.
Yu, Z., Tang, Y., Cai, G., Ren, R., Tang, D., 2019. Anal. Chem. 91, 1222-1226.
Zhang, B.H., Pan, X.P., Cobb, G.P., Anderson, T.A., 2007. Dev. Biol. 302, 1-12.
Zhang, L., Ding, B.Z., Chen, Q.H., Feng, Q., Lin, L., Sun, J.S., 2017. Trac-Trends Anal. Chem. 94, 106-116.